PHYSICS

Strongly correlated multielectron bunches from interaction with quantum light

Suraj Kumar[1]†, Jeremy Lim[2]†, Nicholas Rivera[3], Wesley Wong[1], Yee Sin Ang[2], Lay Kee Ang[2], Liang Jie Wong[1]*

Strongly correlated electron systems are a cornerstone of modern physics, being responsible for groundbreaking phenomena from superconducting magnets to quantum computing. In most cases, correlations in electrons arise exclusively because of Coulomb interactions. In this work, we reveal that free electrons interacting simultaneously with a light field can become highly correlated via mechanisms beyond Coulomb interactions. In the case of two electrons, the resulting Pearson correlation coefficient for the joint probability distribution of the output electron energies is enhanced by more than 13 orders of magnitude compared to that of electrons interacting with the light field in succession (one after another). These highly correlated electrons are the result of momentum and energy exchange between the participating electrons via the external quantum light field. Our findings pave the way to the creation and control of highly correlated free electrons for applications including quantum information and ultrafast imaging.

INTRODUCTION

The interaction of free electrons with light forms the basis of important imaging paradigms such as cathodoluminescence microscopy (*1*–*4*), electron energy-loss spectroscopy (*1*, *3*–*12*), and, photon-induced near-field microscopy (PINEM) (*3*, *4*, *11*, *13*–*24*). In addition to revealing the most fleeting dynamics of matter and radiation down to subatomic length scales, free electron–light interactions have also been leveraged as a versatile method for shaping both the output free electron wave function (*3*, *11*, *13*–*20*, *25*–*37*) and the emitted radiation (*2*, *38*–*56*).

Recent works have shown that it is possible to induce electron-electron entanglement (*47*), realize nontrivial quantum states of light (e.g., squeezed states and displaced Fock states) (*57*), use exchange mechanisms between free electrons to possibly create single attosecond electron pulses (*58*), and entangle distant photons (*54*) by subjecting photonic states to multiple successive interactions with quantum electron wave packets (QEWs) in quantum PINEM (QPINEM) setups. It should be emphasized that in these cases, each QPINEM interaction involves only a single-electron QEW. Recently, correlations between multiple QEWs arising as a result of Coulomb interactions have been explored theoretically and experimentally (*59*, *60*). However, Coulomb interactions leads to only one specific type of correlation in which the electrons repel each other in physical space as much as possible. The question arises as to whether there might be complementary ways of tailoring correlations between multiple free electrons.

Here, we show that strong correlations between multiple QEWs can be created and tailored when multiple QEWs interact with a quantized photon field—even in the absence of Coulomb interactions. Instead, the quantized energy of the external photon field unexpectedly becomes a means of interparticle interaction between the individual electrons. The individual electrons can thus trade quanta of momentum and energy with each other even when they are too far spaced for Coulomb interactions to matter—we refer to this phenomenon as simply "interelectron momentum exchange" in the rest of this paper for brevity. We show that interelectron momentum exchange results in output electrons that are highly correlated in energy. Specifically, we show that the Pearson correlation coefficient (PCC) of the energies of the participating electrons is enhanced by more than 13 orders of magnitude compared to the correlation that already exists from the free electrons interacting with the photon mode in succession (one after another) where PCC is a measure of linear correlation which takes on values between −1 and 1. A PCC value close to 1 indicates strong linear correlation between two quantities i.e., increasing one also increases the other. A PCC value close to −1 on the other hand indicates that increasing one quantity is correlated with the decrease in the other. Last, we show that postselecting an electron in a multi-QEW interaction with quantum light is a robust way of tailoring electron-electron correlations in energy. The electrons after interaction exhibit varied correlation patterns. Our findings show that interelectron momentum exchange could provide the means to correlate and entangle large numbers of electrons with a photon field and shape free electron correlations for applications like ultrafast imaging and quantum information science.

RESULTS

We consider an interaction with N QEWs interacting with a single photon mode. We make the assumptions (conventional for PINEM and other free electron–light interactions) that the electrons are (i) monoenergetic (unshaped), (ii) traveling through a charge-free region ignoring Coulombic effects, and that (iii) their momenta are much stronger than the electromagnetic vector potential $\vec{A}$ (*14*). To model an interaction between N QEWs with a single-photon mode, we use the interaction Hamiltonian (in the Schrodinger picture, see Methods)

$$\hat{\mathscr{H}}_{\text{int}} = \sum_{\mu \in \mathbb{Z}^+} (g_\mu \hat{a}^\dagger \hat{b}_\mu + g_\mu^* \hat{a} \hat{b}_\mu^\dagger) \tag{1}$$

[1]School of Electrical and Electronic Engineering, Nanyang Technological University, 50 Nanyang Avenue, Singapore 639798, Singapore. [2]Science, Mathematics and Technology, Singapore University of Technology and Design, 8 Somapah Road, Singapore 487372, Singapore. [3]Department of Physics, Harvard University, Cambridge MA 02138, USA.
*Corresponding author. Email: liangjie.wong@ntu.edu.sg
†These authors contributed equally to this work.

where the subscript $\mu \in \mathbb{Z}^+$ indicates that the respective quantity is associated with the electron μ and g_μ is the electron-photon coupling strength. The photon ladder operators $\hat{a}$ and $\hat{a}^\dagger$ act on Fock states in the usual way: $\hat{a}|n\rangle = \sqrt{n}|n-1\rangle$, $\hat{a}^\dagger|n\rangle = \sqrt{n+1}|n+1\rangle$, where n is the number of photons in the Fock state. The ladder operator $\hat{b}_\mu$ ($\hat{b}_\mu^\dagger$) decrements (increments) the electron state $|j\rangle$: $\hat{b}|j\rangle = |j-1\rangle$, $\hat{b}^\dagger|j\rangle = |j+1\rangle$ where an electron in eigenstate $|j\rangle$ has energy $E_j = E_0 + j\hbar\omega_0$, $j \in \mathbb{Z}$, E_0 is the initial electron energy and $\hbar\omega_0$ is the photon energy. It should be noted that the electron ladder operators commute with each other: $[\hat{b}, \hat{b}^\dagger] = 0$. The corresponding scattering operator (see Methods) is given by

$$\begin{aligned}\hat{S}_N = e^{\frac{1}{2}\left(\sum_\mu |G_\mu|^2\right)} e^{-G_N^* \hat{b}_N^\dagger \hat{a}} \ldots e^{-G_1^* \hat{b}_1^\dagger \hat{a}} \\ \times e^{G_1 \hat{b}_1 \hat{a}^\dagger} \ldots e^{G_N \hat{b}_N \hat{a}^\dagger} \\ \times e^{\frac{1}{2}\sum_{\mu<\nu}\left(G_\mu G_\nu^* \hat{b}_\mu \hat{b}_\nu^\dagger + h.c.\right)}\end{aligned} \tag{2}$$

where $G_\mu \equiv -i\frac{g_\mu \tau}{\hbar}$ is the dimensionless electron-photon coupling strength term and τ is the interaction time. In the case of two QEWs, this reduces to

$$\begin{aligned}\hat{S}_2 = e^{\frac{1}{2}(|G_1|^2+|G_2|^2)} \overbrace{e^{-G_1^* \hat{b}_1^\dagger \hat{a}} e^{-G_2^* \hat{b}_2^\dagger \hat{a}} e^{G_1 \hat{b}_1 \hat{a}^\dagger} e^{G_2 \hat{b}_2 \hat{a}^\dagger}}^{\text{PINEM terms}} \\ \times \underbrace{e^{\frac{1}{2}G_1 G_2^* \hat{b}_2^\dagger \hat{b}_1} e^{\frac{1}{2}G_1^* G_2 \hat{b}_2 \hat{b}_1^\dagger}}_{\text{interelectron momentum exchange}}\end{aligned} \tag{3}$$

where $\hat{S}_2$ acts on the three-body (one photon and two electrons) state $|n, j, k\rangle$, n is the number of photons, and j (k) labels the units of energy gain for electron 1 (electron 2). For an arbitrary initial state $\sum_{n_i j_i k_i} C^{(0)}_{n_i j_i k_i} |n_i, j_i, k_i\rangle$, where $\left|C^{(0)}_{n_i j_i k_i}\right|^2$ is the probability of finding the initial state in $|n_i, j_i, k_i\rangle$, and the probability of obtaining a final state $|n_f, j_f, k_f\rangle$ is given by $P_{n_f j_f k_f} = \left|\sum_{n_i j_i k_i} C^{(0)}_{n_i j_i k_i} S^{n_f j_f k_f}_{n_i j_i k_i}\right|^2$. Here, $S^{n_f j_f k_f}_{n_i j_i k_i} \equiv \langle n_f, j_f, k_f | \hat{S}_2 | n_i, j_i, k_i \rangle$ is the S-matrix element (see Eq. 11 in Methods for full expression), and the subscripts "i" ("f") denote the initial (final) quantities. Note that Eq. 3 is nonperturbative in the electron-photon coupling strength.

In addition to the usual interaction terms (overbraced terms in Eq. 3) found in QPINEM interactions that describe electron-photon energy exchange, it is noteworthy that terms describing interelectron momentum exchange arise (underbraced terms in Eq. 3). This implies that both electrons can affect each other even in the absence of Coulomb interactions. Physically, the interelectron momentum exchange terms can be understood as such: Both electrons separately emit and absorb photons, resulting in changes to the photon field itself. In turn, these changes allow both electrons to affect each other. Because each of the interelectron momentum exchange terms scales as $|G_1 G_2|$, we expect the exchange terms to become comparable in strength to the QPINEM terms when $|G_1| \sim |G_2| \sim |G_1 G_2| \sim 1$—this is the regime we explore. Physically, this corresponds to the regime in which the electron has a high probability of emitting or absorbing one photon, and so there is also a substantial probability of one electron absorbing/emitting a photon generated by the other electron. We compare the photon and electron distributions for one-QEW and two-QEW interactions with quantized light in the Supplementary Materials, section S1.

In this regime, we can study the effects of interelectron momentum exchange in interactions between multielectron pulses and quantized light. In Fig. 1, we have considered the case where two electrons interact with a quantized photon field successively in Fig. 1 (A and B) and then simultaneously in Fig. 1 (C and D). Unlike the successive QEWs, the simultaneous QEWs exchange energy and momentum mediated via the light field. The corresponding joint probability distribution map of final energies of the QEWs is shown for the successive and simultaneous cases in Fig. 1 (B and D, respectively). We observe a symmetrical joint probability distribution map in electron energies in the case of simultaneous electrons due to interelectron momentum exchange, resulting in a PCC (see Methods for definition) that is more than 13 orders of magnitude greater than that of the case with successive electrons. Furthermore, the high PCC due to interelectron momentum exchange is a purely quantum phenomenon in the sense that the high PCC manifests only when light is treated as a quantum object. The low values are not a numerical artifact but a manifestation of nonzero correlation. Some correlation would generally exist in the successive case, except in the limit of an infinite number of photons, because the finite number of photons in the mode generally leads to altered photon statistics seen by electron 2, after electron 1 has interacted with the mode. In other words, because the interaction of electron 1 with the photon field determines the photon field that electron 2 then interacts with, it is not unexpected that a nonzero (though generally residual) correlation exists between electron 1 and electron 2 even in the successive case. The upper limit of any PCC is always one. PCC = 1 is in principle possible, but the conditions to realize this remain a topic of future research. Our findings suggest that we can design an optical mode and electron energy distribution to increase PCC using numerical optimization techniques—by varying parameters such as the coupling strength, the initial photon number and the interaction time. We compare the PCC for two-QEW simultaneous interactions when light is a nonquantized field and when light is quantized as shown in Fig. 1 (E and F). We observe that the interaction with nonquantized light does not generate high PCC. In contrast, when the light field is treated as a quantum object, we observe high PCC. For the derivation of the scattering matrix element for a two-QEW interaction with a classical light field, refer to Supplementary Materials section S2.

Let us now answer the question: Under what conditions would the quantized light case approach the case of interacting with nonquantized light, causing interelectron momentum exchange induced correlations to vanish? We can define the nonquantized limit for a quantum multielectron interaction with a light field as one where the energy exchanged by the electrons does not substantially alter the light field state; thus, the light field behaves as a reservoir. This corresponds to $N_p \gg |G|^2$ where N_p is the number of photons and G is the electron-photon dimensionless coupling. In Fig. 2, we see that for large N_p and low G, both the case with simultaneous electrons in Fig. 2A and the case with successive electrons in Fig. 2B correlations approach a similar squarish pattern, which is also what is obtained when performing the simulations with the nonquantized light field. Supplementary Materials section S3 contains a more detailed comparison of the quantized

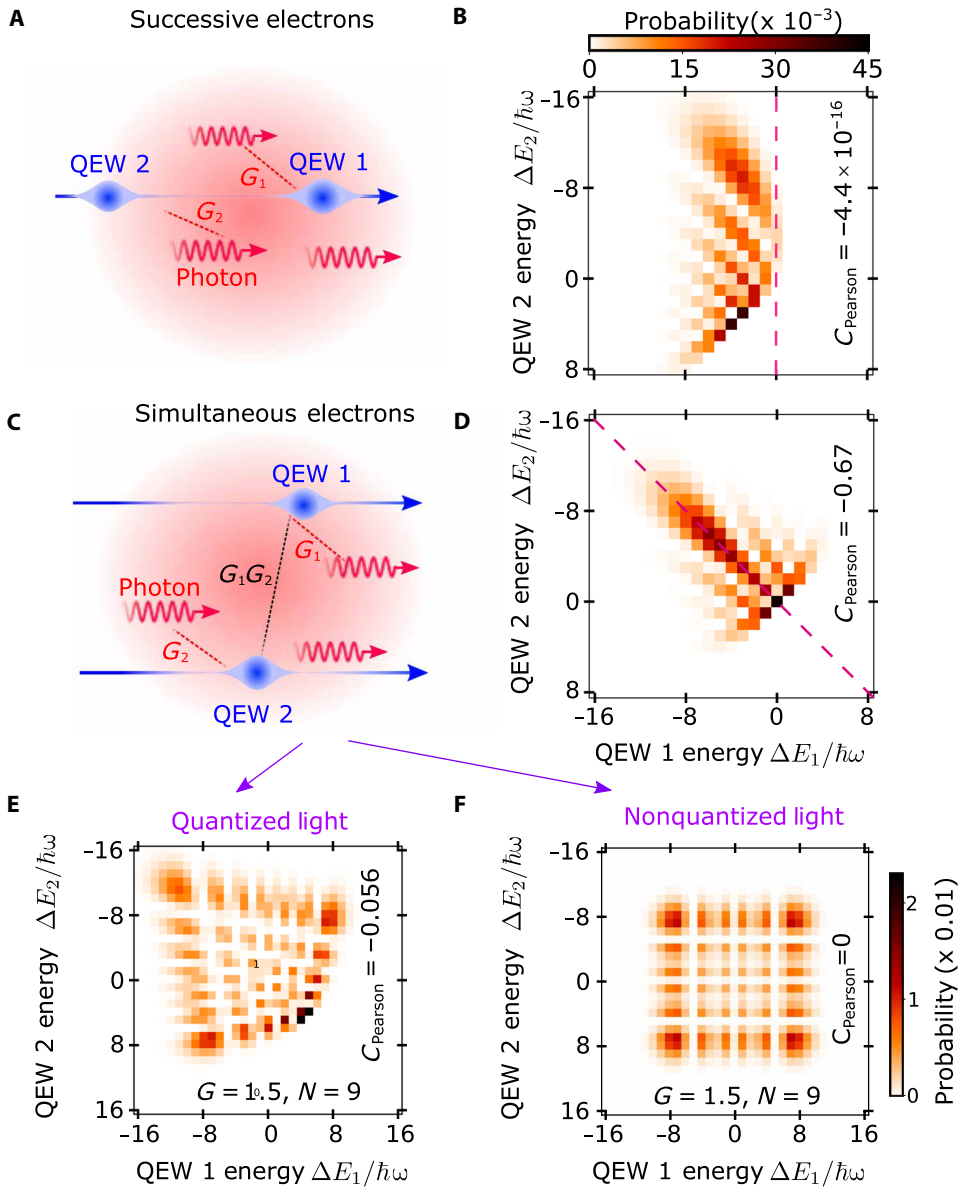

Fig. 1. Simultaneous interaction of two free electron QEWs with quantized light produces highly correlated electrons. We consider a light field prepared in the vaccum Fock state, through which two QEWs are passed. These QEWs, hereafter referred to as QEW 1 and QEW 2, couple to photons with dimensionless strengths $G_1 = 2$ and $G_2 = 2$, respectively. (**A**) In a quantum two-electron–light interaction without interelectron momentum exchange, the QEWs pass through an electromagnetic environment one after the other successively. QEW 1 exchanges energy with the quantized light field with the restriction that the final photon number be non-negative. QEW 2 then interacts with the changed light field, and we measure the energy of both electrons. (**B**) The joint probability distribution of the energy gain of QEW 1 and QEW 2, respectively, is shown here for the successive case. We see that because of the restriction on QEW 1, the probability is zero for any increase in its energy (beyond pink dotted line). The distribution is also asymmetrical and the PCC is of the order 10^{-16}. (**C**) In the simultaneous case, the two QEWs interact simultaneously with the quantized light field. (**D**) We show the QEW energy gain joint distribution for the simultaneous case. The joint distribution shows symmetry along the pink dotted line. The PCC is 0.67 in magnitude and 15 orders of magnitude larger compared to the successive case. (**E** and **F**) We compare the correlation in energy between QEW 1 and QEW 2 for simultaneous interaction with (E) quantized light and (F) nonquantized light, showing that the phenomenon of enhanced PCC by interelectron momentum exchange is enabled by the quantum nature of light. Here, we have fixed the average photon number to be 9 and the coupling constant to be $G = 1.5$.

and nonquantized light field cases and how the latter approaches the former in the limit of low N_p and large G. We also notice that correlation of the QEWs for simultaneous QEW interactions (Fig. 2A) is strong for low N_p and large G.

Apart from getting high PCC as a result of interelectron momentum exchange between QEWs, we can further tailor correlations by postselecting one of the participating QEWs. In Fig. 3, we show a schematic to postselect an electron (or more) in a simultaneous interaction between N QEWs and a photon Fock state. As shown in Fig. 3A, we can postselect QEW 1 to be at a certain energy corresponding to normalized energy gain k_1 and then measure the correlation in energy between QEW 2 and QEW 3. Figure 3 (B to D)

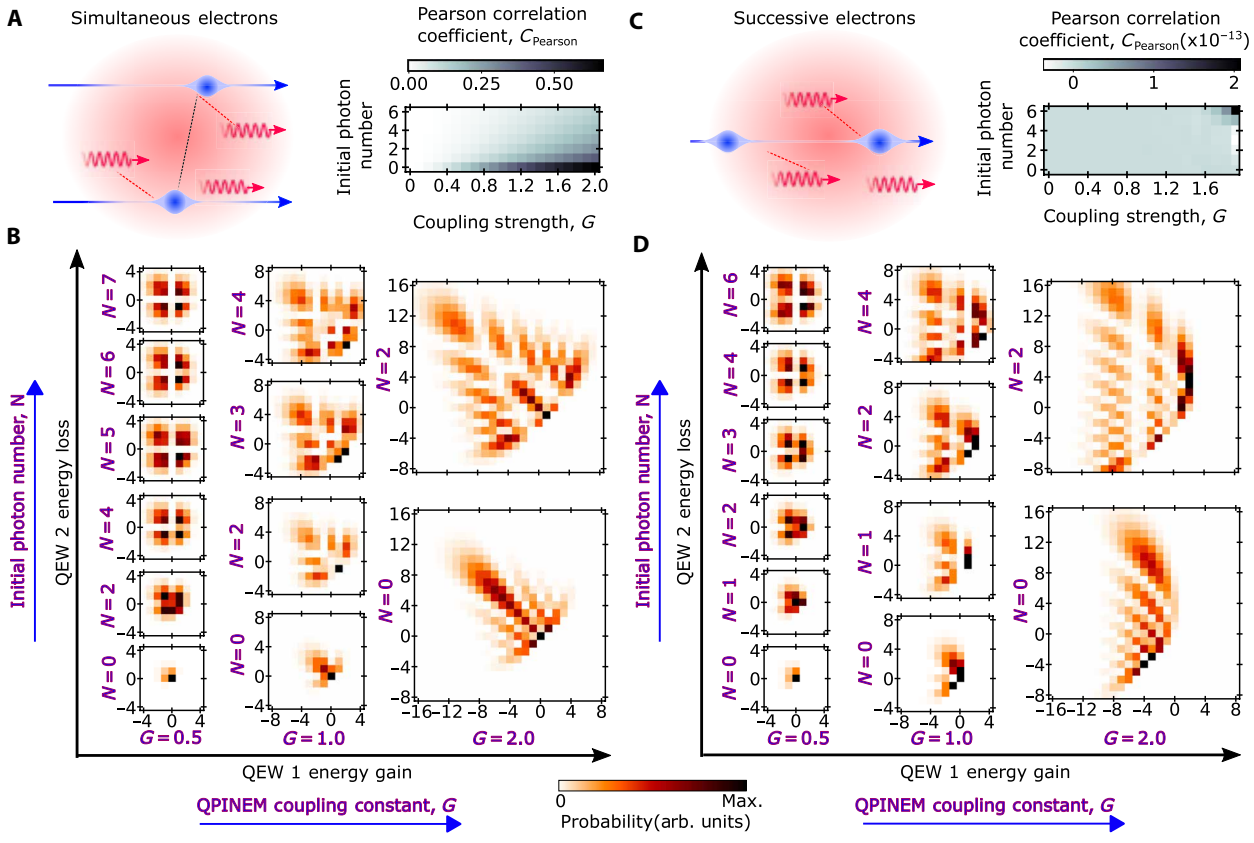

Fig. 2. Stronger correlations in the output electrons are favored by lower initial photon numbers and larger interaction strengths. (**A**) We show the case of simultaneous electrons with interelectron momentum exchange and plot the colormap for the PCC with varying coupling strength *G* and initial photon number. Note that because all PCC values here are negative, we plot the absolute value. (**B**) We display energy correlation plots after interaction for the case of two QEWs interacting with quantized light as we vary the interaction strength and photon number in the presence of interelectron momentum exchange. We see that as photon number increases, especially for low interaction strength, the plots approach the nonquantized limit and become more square-like. However, for larger interaction strength, it takes a much larger photon threshold for the plot to approach the nonquantized light case. (**C**) For completeness, we show the case without interelectron momentum exchange with the corresponding joint probability distribution map for the PCC. (**D**) We observe that for low interaction strength and high photon number, the plot similar to (B) approaches the nonquantized light case. We can thus designate a regime for which both cases tend to the behavior expected from interactions with nonquantized light. At higher interaction strengths, the plots deviate from the nonquantized light case as expected. In general, the correlation grows weaker as we increase average photon number and grows stronger as we increase interaction strength.

shows that postselection of QEW 1 results in highly correlated QEWs whose joint probability distribution map can be modified. For instance, postselecting for higher QEW 1 energies shifts the distribution map in favor of larger photon number and larger QEW energy loss. The resulting pattern of the energy correlation is also distinct from what we can obtain from the two-QEW cases considered in Fig. 2. In Fig. 3 (E and F), we postselect two QEWs of four QEWs that interact simultaneously with the light field and show the varied patterns that emerge for different postselected energies. In Supplementary Materials section S4, we show that the postselection result remains the same if the energies of two postselected QEWs are interchanged, which is not a surprise because the QEWs are indistinguishable.

It should be noted that the two-electron interaction theory in (*47*) is the study of the sequential interaction of electrons with a quantized light field where one cannot observe interelectron momentum exchange between the electrons. The interaction of the electrons with the quantized light field studied in this work generalizes the interaction theory in (*47*) to any number of free electrons interacting with the quantized light field and investigates the resulting phenomenon of interelectron momentum exchange. Our results show that the photon and QEWs are entangled with each other, a conclusion also reached by recent works for the case of sequential free electrons interacting with a quantized light field (*47*) and for the case of a single free electron interacting with multiple quantized light fields used to predict previously unknown quantum optical states by (*57*). Our results here show that the entanglement persists even in our case when the free electrons interact simultaneously with quantized light fields. Thus, entanglement occurs even if the electrons are interacting with the light field at the same time instead of in succession.

DISCUSSION

It is important to note that the high correlations due to field-mediated interelectron momentum exchange terms have no equivalent in theory that considers a nonquantized field (Supplementary Materials, section S2). This is consistent with our theory when we

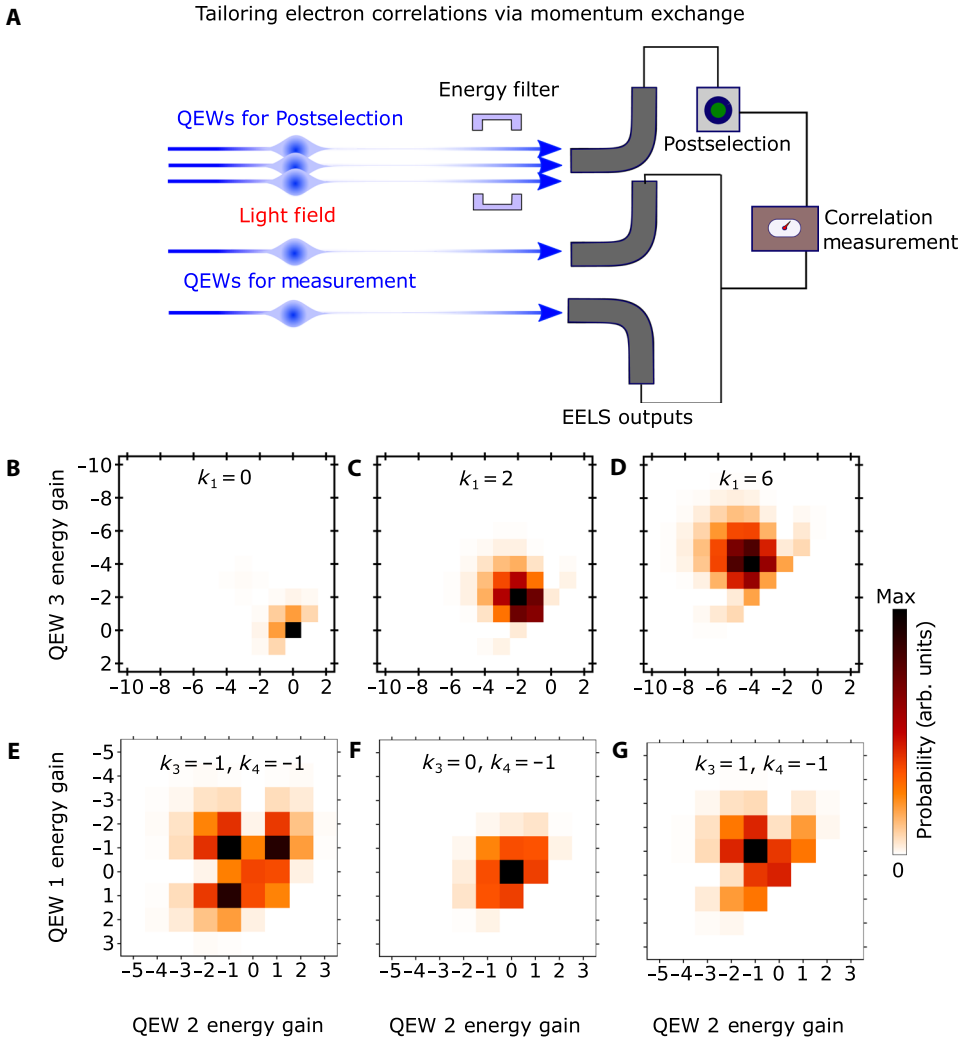

Fig. 3. Tailoring strong correlations between electrons in energy space via postselection. (**A**) We show the schematic of a multi-QEW interaction with interelectron momentum exchange. We postselect a subset of the QEWs for certain energies. Note that in the case of interelectron momentum exchange, all electrons are identical as far as the interaction is concerned. We then measure the rest of the QEWs and plot their energy correlations. EELS, electron energy-loss spectroscopy. (**B** to **D**) We plot the correlation plots in the case of interelectron momentum exchange when we postselect any one of three electrons, i.e. QEW 1 with energy k_1 to gain 0, 2, and 6 quanta of energy, respectively. We observe that postselection in the presence of interelectron momentum exchange can produce highly correlated symmetric correlations between free electrons. Moreover by changing the postselected energy we can shift the correlations along the symmetry axis of the distribution. The coupling strengths for all cases has been set to 1 and the initial photonic state is the vaccum Fock state. (**E** to **G**) We postselect any two QEWs (here QEW 3 and QEW 4) for energies k_3 and k_4, respectively, and plot energy correlations between QEW 1 and QEW 2 for $k_4 = -1$, $k_3 = -1, 0, 1$.

consider an initial photon distribution described as a coherent state $|\alpha\rangle$ in the limit $|\alpha|^2 = n_{av} \gg 1$ and $|G|^2 \ll 1$ (proof in Supplementary Materials, section S3). However, within the strong-coupling regime (high coupling strength) of interaction of free electrons with quantized light, our results show that these interelectron momentum exchange terms give rise to substantial enhancements in the correlations (as measured by PCC) between participating QEWs. We note that the strong coupling regime is currently seen as a promising regime in which highly nonclassical states of light can be generated, shaped, and probed by free electrons (*54*–*57*), and the effect of simultaneous interaction on the production of such optical states is an exciting direction of inquiry. While we have used the example of Fock state for the light field in all our simulations in the main text, Supplementary Materials section S5 contains simulations for the cases where the light field is a coherent or thermal light field with the correlations still remaining strong.

Crucially, a recent experiment (*61*) has shown that two-electron QEWs can already be generated using currently available electron sources (*62*–*66*). This suggests that our scheme involving two-electron QEWs is already within experimental reach. Advances in electron source technologies, coupled with the results we present here, motivate the study of unprecedented non-Coulombic effects in QPINEM and other free electron–light interactions involving multielectron QEWs with quantum states of light. In Supplementary Materials section S6, we present experimental

plans for demonstrating interelectron momentum exchange under currently achievable experimental parameters.

In the field of quantum computing, the strong nonlocal entanglement of particles has been studied as part of an effort to realize scalable quantum computation systems that enable parallel quantum computing (*67*). We note that interelectron momentum exchange is a phenomenon that is nonlocal compared to say, Coloumb interactions, and can potentially entangle an arbitrarily large number of electrons with a single photon field—which is not possible with Coulomb interaction because of the repulsive nature of Coulomb forces that limits the number of electrons that can be placed in a limited volume of space. The use of free electrons for quantum computing has several unique advantages over using photon-based or bound electron–based systems. Free electrons readily propagate information across macroscopic distances and are thus a potential candidate for "flying qubits" (*68*, *69*), for instance via the phenomenon of free electron–polariton blockade, made possible by leveraging quantum recoil (*70*, *71*). These flying qubits are a core component of designing a potential quantum network or quantum internet, which has motivated implementations thus far in semiconductor systems and bound-electron systems (*68*). The photon-mediated interelectron momentum exchange mechanism we introduce in this work then empowers the paradigm of using free electrons as flying qubits, by providing a way to correlate multiple flying qubits and potentially to design free electron–based protocols complimenting recent work that have used free electron–light interactions to implement a free electron–based protocol (*72*). In our photon-mediated interelectron momentum exchange mechanism, the control of the photon mode is crucial as the statistics of the initial photon mode provides an extra degree of freedom in controlling the entanglement. Using free electrons as flying qubits, we could impart information to stationary qubits in the form of photonic states, as has already been shown in the literature (*22*, *57*).

In this work, we have considered examples with up to four electrons; however, our theory accommodates an arbitrary number of electrons interacting with light. We note that there arises an interelectron momentum exchange term for each electron pair in a multi-QEW interaction. As the number of electrons in a multielectron pulse increases, Coulombic pairwise interactions may also increasingly become substantial. Recent work (*59*, *63*) has shown that electron-electron correlations arising from Coulombic interactions can affect shot noise, electron drift, etc. in the absence of a light field. In the regime where these Coulombic interactions are substantial, they will coexist with interelectron momentum exchange. In such cases, the relative magnitude of the electron-light coupling to the electron-electron coupling will determine which phenomenon dominates. In low-photon simultaneous interactions with quantum light, we expect electron correlations to favor the electrons losing energy as opposed to the expectation from Coloumbic interactions alone. Above all, we note that the physical origins of Coulomb interactions and interelectron momentum exchange are very distinct in nature: Coulomb interactions arise from the exchange of virtual photons between QEWs, whereas interelectron momentum exchange arises from the exchange of physical photons.

The impact of shaping the QEWs on the interelectron exchange phenomenon is an intriguing prospect for future work. Shaping the QEWs introduces quantum interference (*24*), which should also coexist with interelectron momentum exchange and potentially lead to even more versatility in shaping electron-electron correlations and entanglement compared to the unshaped case.

In summary, we show that simultaneous interactions involving multielectron QEWs allow us to tailor electron-electron energy correlations in ways that go beyond what successive single-electron QEW interactions are capable of. Specifically, the use of multielectron pulses result in the appearance of interelectron momentum exchange—the exchange of energy and momentum between QEWs even in the absence of Coulombic forces. We have shown that interelectron momentum exchange is a purely quantum phenomenon, manifesting only in regimes where the quantum nature of light is relevant. As a result of interelectron momentum exchange, outgoing two-QEW pulses have PCC more than 13 orders of magnitude larger than those obtained when the QEWs interact with the photon mode in succession. We have also shown that interelectron momentum exchange is a robust means of creating and tailoring strong many-QEW correlations in energy, especially with the use of post-selection techniques. The photon-mediated interelectron momentum exchange we have studied thus provides an unprecedented means of strongly correlating large numbers of free electrons in energy-momentum space, even if these electrons are spaced far apart enough that Coulombic interactions are no substantial. Our findings fill an important gap in the understanding of multielectron interaction with photons and pave the way toward many-electron entanglement techniques for applications like quantum information and ultrafast imaging.

METHODS

Physical model for interaction of multiple QEWs with photons

Here, we derive the scattering operator describing the nonperturbative interaction between N paraxial QEWs simultaneously interacting with a common photon mode, as well as the S-matrix element. We assume that all electrons do not interact directly through the Coulomb near-field, which is justified for electron pulses with low electron densities. We also assume there are no other external charges and that the electromagnetic vector potential is much smaller than the electron energies. The full Hamiltonian is given by

$$\widehat{\mathscr{H}}_{\text{total}} = \widehat{\mathscr{H}}_{\text{l}} + \widehat{\mathscr{H}}_{\text{e}} + \widehat{\mathscr{H}}_{\text{int}} \tag{4}$$

where $\widehat{\mathscr{H}}_{\text{total}}$ is the complete Hamiltonian, $\widehat{\mathscr{H}}_{\text{l}}$ is the Hamiltonian term for the light field alone, $\widehat{\mathscr{H}}_{\text{e}}$ is the Hamiltonian term for the N electrons, and $\widehat{\mathscr{H}}_{\text{int}}$ is the interaction Hamiltonian term. The expressions for the light and electrons' Hamiltonian terms in the Schrodinger picture are given by

$$\widehat{\mathscr{H}}_{\text{l}} = \left(\hat{a}^{\dagger}\hat{a} + \frac{1}{2}\right)\hbar\omega_0, \quad \mathscr{H}_{\text{e}} = \sum_{\mu} \hat{P}_{\mu} v_{\mu} \tag{5}$$

where $\hat{a}(\hat{a}^{\dagger})$ is the annihilation(creation) photon operator satisfying $[\hat{a}, \hat{a}^{\dagger}] = 1$, ω_0 is the frequency of the light field, and $\hat{P}_{\mu}$ and v_{μ} are the momentum operator and speed of the electron indexed by μ. The interaction Hamiltonian, which we use to compute the scattering operator, is given by Eq. 1. We obtain the scattering operator from the interaction Hamiltonian as

$$S_N = e^{\sum_{\mu=1}^{N} (G_\mu \hat{b}_\mu \hat{a}^\dagger - G_\mu^* \hat{b}_\mu^\dagger \hat{a})} \tag{6}$$

Using the Baker-Campbell-Hausdorff formula and separating the hermitian conjugate terms, we obtain Eq. 3. Reducing this to the case of two electrons ($N = 2$), we recover Eq. 3. Note that interelectron momentum exchange occurs between both electrons despite no interaction between them due to Coulombic forces. The interelectron momentum exchange factors arise as a direct result of the nonvanishing commutator $[\hat{a}, \hat{a}^\dagger] = 1$, and implies that the interelectron momentum exchange is mediated by the photon field. We now assume that the two electrons QEW 1 and QEW 2 are monoenergetic with initial energies $j_i\hbar\omega$ and $k_i\hbar\omega$, respectively, with j_i and k_i being the quantum numbers defining the electron energies. In the examples used in the text, we also assume that the light field is initially in a Fock state with number of photons given by n_i. The initial state of the three-body system is thus given by $|n_i, j_i, k_i\rangle$. Similarly, we indicate the final state of the system as $|n_f, j_f, k_f\rangle$. We define the S-matrix element used to calculate the transition probability between the initial and final states to be

$$S^{n_f,j_f,k_f}_{n_i,j_i,k_i} \equiv \langle n_f, j_f, k_f | \hat{S}_2 | n_i, j_i, k_i \rangle \tag{7}$$

where n_i is the initial number of which we solve by expanding the exponential operators in their series expansions. We obtain

$$\begin{aligned} S^{n_f,j_f,k_f}_{n_i,j_i,k_i} &= e^{\frac{1}{2}(|G_1|^2+|G_2|^2)} \\ &\times \sum_{l,m,p,q,r,s} \sqrt{\frac{(n_i+l+q)!(n_f+m+p)!}{n_i!n_f!}} \\ &\times \frac{G_1^q G_2^l (-G_1^*)^m (-G_2^*)^p}{l!m!p!q!} \frac{(G_1 G_2^*)^r (G_1^* G_2)^s}{r!s!2^{r+s}} \\ &\times \langle n_f+m+p | n_i+l+q \rangle \\ &\times \langle j_f-m+r, k_f-p-r | j_i-q+s, k_i-l-s \rangle \end{aligned} \tag{8}$$

where integers $l, m, p, q, r, s \in [0, \ldots, \infty)$. Here, we have split the inner product on the three-body space as the product of two other inner products on the QEWs' space and photon space, respectively, for legibility. The inner products are Kronecker deltas that enforce the following conditions

$$\begin{aligned} \Delta n + m + p &= l + q, \\ \Delta k - p - r &= -l - s, \\ \Delta j - m + r &= -q + s \end{aligned} \tag{9}$$

Here, $\Delta k \equiv k_f - k_i$, $\Delta j \equiv j_f - j_i$, and $\Delta n \equiv n_f - n_i$ are the differences between the initial and final quantum numbers. Using all three relations gives us the energy conservation relation

$$\Delta n + \Delta j + \Delta k = 0 \tag{10}$$

From the first two conditions in Eq. 10, all dependencies on indices q and l vanish, allowing us to obtain the final expression for the S-matrix element

$$\begin{aligned} S^{n_f,j_f,k_f}_{n_i,j_i,k_i} &= e^{\frac{1}{2}(|G_1|^2+|G_2|^2)} \frac{G_1^{-\Delta j} G_2^{-\Delta k}}{\sqrt{n_i!n_f!}} \times \\ &\sum_{m,p,r,s} \frac{(-|G_1|^2)^m (-|G_2|^2)^p (n_f+p+m)!}{m!p!(s-r+m-\Delta j)!(p-\Delta k-s+r)!} \\ &\frac{|G_1|^{2s} |G_2|^{2r}}{r!s!2^{r+s}} \end{aligned} \tag{11}$$

Note that because $q, l \geq 0$, it follows that $(p - \Delta k - s + r) \geq 0$ and $(s - r + m - \Delta j) \geq 0$. For computational efficiency, we find it favorable to use the S-matrix expression with $\hat{a}^\dagger$ terms on the left hand side and the $\hat{a}$ terms on the right hand side (c.f. Eq. 3)

$$\begin{aligned} \hat{S}_2 &= e^{-\frac{1}{2}|G_1|^2} e^{-\frac{1}{2}|G_2|^2} e^{G_1 \hat{b}_1 \hat{a}^\dagger} e^{G_2 \hat{b}_2 \hat{a}^\dagger} e^{-\frac{1}{2} G_1 G_2^* \hat{b}_2^\dagger \hat{b}_1} \\ &\times e^{-\frac{1}{2} G_1^* G_2 \hat{b}_2 \hat{b}_1^\dagger} e^{-G_1^* \hat{b}_1^\dagger \hat{a}} e^{-G_2^* \hat{b}_2^\dagger \hat{a}} \end{aligned} \tag{12}$$

Repeating the steps above, we arrive at

$$\begin{aligned} S^{n_f,j_f,k_f}_{n_i,j_i,k_i} &= e^{-\frac{1}{2}(|G_1|^2+|G_2|^2)} (-G_1^*)^{\Delta j} (-G_2^*)^{\Delta k} \sqrt{n_i!n_f!} \\ &\times \sum_{m,p,r,s} \frac{(-|G_1|^2)^s (-|G_2|^2)^r}{(n_f-m-p)!r!s!2^{r+s}} \\ &\times \frac{(-|G_1|^2)^m (-|G_2|^2)^p}{m!p!} \\ &\times \frac{1}{(\Delta j+m+s-r)!(\Delta k+p+r-s)!} \end{aligned} \tag{13}$$

where $r, s \in [0, \ldots, \infty)$, and the other indices have the following bounds

$$\begin{aligned} 0 \leq p &\leq n_f - m, \\ 0 \leq m &\leq n_f, \\ \max\{0, -\Delta j - m + r\} &\leq s \leq \Delta k + p + r \end{aligned} \tag{14}$$

The first relation comes from the requirement that $(n_f - m - p) \geq 0$. Because $p \geq 0$, it follows that $n_f - m \geq 0$, which is the second relation. The third relation is obtained by imposing $(\Delta j + m + s - r) \geq 0$ and $(\Delta k + p + r - s) \geq 0$. We see that three indices are bounded from above as opposed to Eq. 11, where only r-s is bounded. Hence, Eq. 13 affords us much greater computational efficiency.

We can show that Eq. 11 reduces to the expression for a single-QEW interaction with quantum light (*47*)

$$\begin{aligned} S^{n_f,j_f}_{n_i,j_i} &= \langle n_f, j_f | \hat{S} | n_i, j_i \rangle \\ &= \frac{e^{\frac{1}{2}|G|^2} G^{\Delta n}}{\sqrt{n_f!n_i!}} \sum_{m=0}^{\infty} \frac{(-|G|^2)^m}{m!(m+\Delta n)!} (n_f+m)! \end{aligned} \tag{15}$$

subject to the energy conserving relation

$$\Delta j + \Delta n = 0 \tag{16}$$

which is consistent with the expression presented in (*47*).

The PCC is a measure of linear correlation between two quantities (in our case, the electrons' final energies). A high PCC—namely, a large linear correlation—implies that measuring one of the electrons would result in a high probability of knowing the other electron's

energy. Our choice of PCC thus serves two purposes: first, as a fundamental characteristic of interelectron momentum exchange, which can serve as the signature of this phenomenon in an experimental measurement; second, as a valuable property that can be leveraged in applications such as coincidence detection, which uses correlations between multiple particles to reduce or eliminate the background noise in a measurement. Coincidence detection setups involving correlated photon pairs and correlated photon-electron pairs have been previously proposed and demonstrated in the literature (*73*–*76*). Here, our ability to generate highly correlated electron-electron pairs paves the way to a coincidence measurement scheme based on these correlated electrons. The large, 13 order-of-magnitude difference implies that the difference in PCC would be relatively easy to measure, requiring a low electron count of about 30, and that the PCC would thus serve as an easily observable, distinctive signature of the interelectron momentum exchange phenomenon.

Given two probability distributions $P(x)$ and $Q(x)$ defined over the same space X where $x \in X$, we define the PCC as

$$\mathrm{PCC}(P,Q) = \frac{\langle (P - \langle P \rangle)(Q - \langle Q \rangle) \rangle}{\sigma_P \sigma_Q} \tag{17}$$

where σ_P is the standard deviation of distribution P and $\langle P \rangle$ is the expectation value of distribution P.

In the context of our work, the relevant distributions are the energies of the final QEWs. The two quantities we are concerned with are QEW 1's energy gain and QEW 2's energy loss after interacting with quantized light denoted by j_f and $-k_f$. We thus calculate the PCC as follows

$$\begin{aligned} \mathrm{PCC}_{e1,e2} &= \frac{\langle (j_f - \langle j_f \rangle)(-k_f - \langle -k_f \rangle) \rangle}{\sigma_{j_f} \sigma_{k_f}} \\ &= -\frac{\langle (j_f - \langle j_f \rangle)(k_f - \langle k_f \rangle) \rangle}{\sigma_{j_f} \sigma_{k_f}} \end{aligned} \tag{18}$$

where $\mathrm{PCC}_{e1,e2}$ is the PCC for the two electrons' final energies, j_f,k_f are the final electron energies of QEW 1 and QEW 2, respectively. The PCC can vary from −1 to +1, and a zero PCC indicates no linear correlation. A negative correlation indicates that QEW 1 gaining energy is correlated with QEW 2 also gaining energy and vice versa.

Supplementary Materials

This PDF file includes:

Sections S1 to S7
Figs. S1 to S7
References

REFERENCES AND NOTES

1. F. J. García de Abajo, Optical excitations in electron microscopy. *Rev. Mod. Phys.* **82**, 209–275 (2010).
2. V. Di Giulio, O. Kfir, C. Ropers, F. J. García de Abajo, Modulation of cathodoluminescence emission by interference with external light. *ACS Nano* **15**, 7290–7304 (2021).
3. M. Liebtrau, M. Sivis, A. Feist, H. Lourenço-Martins, N. Pazos-Pérez, R. A. Alvarez-Puebla, F. J. G. de Abajo, A. Polman, C. Ropers, Spontaneous and stimulated electron–photon interactions in nanoscale plasmonic near fields. *Light Sci. Appl.* **10**, 82 (2021).
4. F. J. García de Abajo, V. Di Giulio, Optical excitations with electron beams: Challenges and opportunities. *ACS Photonics* **8**, 945–974 (2021).
5. J. Verbeeck, S. Van Aert, Model based quantification of eels spectra. *Ultramicroscopy* **101**, 207–224 (2004).
6. J. Verbeeck, H. Tian, P. Schattschneider, Production and application of electron vortex beams. *Nature* **467**, 301–304 (2010).
7. G. Van Tendeloo, S. Bals, S. Van Aert, J. Verbeeck, D. Van Dyck, Advanced electron microscopy for advanced materials. *Adv. Mater.* **24**, 5655–5675 (2012).
8. R. Egoavil, N. Gauquelin, G. T. Martinez, S. Van Aert, G. Van Tendeloo, J. Verbeeck, Atomic resolution mapping of phonon excitations in STEM-EELS experiments. *Ultramicroscopy* **147**, 1–7 (2014).
9. J. Krehl, G. Guzzinati, J. Schultz, P. Potapov, D. Pohl, J. Martin, J. Verbeeck, A. Fery, B. Büchner, A. Lubk, Spectral field mapping in plasmonic nanostructures with nanometer resolution. *Nat. Commun.* **9**, 4207 (2018).
10. A. Polman, M. Kociak, F. J. García de Abajo, Electron-beam spectroscopy for nanophotonics. *Nat. Mater.* **18**, 1158–1171 (2019).
11. C. Liu, Y. Wu, Z. Hu, J. A. Busche, E. K. Beutler, N. P. Montoni, T. M. Moore, G. A. Magel, J. P. Camden, D. J. Masiello, G. Duscher, P. D. Rack, Continuous wave resonant photon stimulated electron energy-gain and electron energy-loss spectroscopy of individual plasmonic nanoparticles. *ACS Photonics* **6**, 2499–2508 (2019).
12. E. Arqué López, V. Di Giulio, F. J. G. de Abajo, Atomic floquet physics revealed by free electrons. *Phys. Rev. Res.* **4**, 013241 (2022).
13. B. Barwick, D. J. Flannigan, A. H. Zewail, Photon-induced near-field electron microscopy. *Nature* **462**, 902–906 (2009).
14. T. S. Park, M. Lin, A. H. Zewail, Photon-induced near-field electron microscopy (pinem): Theoretical and experimental. *New J. Phys.* **12**, 123028 (2010).
15. A. Feist, K. Echternkamp, J. Schauss, S. V. Yalunin, S. Schäfer, C. Ropers, Quantum coherent optical phase modulation in an ultrafast transmission electron microscope. *Nature* **521**, 200–203 (2015).
16. L. Piazza, T. Lummen, E. Quiñonez, Y. Murooka, B. W. Reed, B. Barwick, F. Carbone, Simultaneous observation of the quantization and the interference pattern of a plasmonic near-field. *Nat. Commun.* **6**, 6407 (2015).
17. K. E. Priebe, C. Rathje, S. V. Yalunin, T. Hohage, A. Feist, S. Schäfer, C. Ropers, Attosecond electron pulse trains and quantum state reconstruction in ultrafast transmission electron microscopy. *Nat. Photonics* **11**, 793–797 (2017).
18. G. M. Vanacore, I. Madan, G. Berruto, K. Wang, E. Pomarico, R. J. Lamb, D. McGrouther, I. Kaminer, B. Barwick, F. J. G. de Abajo, F. Carbone, Attosecond coherent control of free-electron wave functions using semi-infinite light fields. *Nat. Commun.* **9**, 2694 (2018).
19. K. P. Wang, R. Dahan, M. Shentcis, Y. Kauffmann, A. B. Hayun, S. Reinhardt, O. Tsesses, I. Kaminer, Coherent interaction between free electrons and a photonic cavity. *Nature* **582**, 50–54 (2020).
20. T. R. Harvey, J.-W. Henke, O. Kfir, H. Lourenço-Martins, A. Feist, F. J. G. de Abajo, C. Ropers, Probing chirality with inelastic electron-light scattering. *Nano Lett.* **20**, 4377–4383 (2020).
21. R. Dahan, S. Nehemia, M. Shentcis, O. Reinhardt, Y. Adiv, X. Shi, O. Be'er, M. H. Lynch, Y. Kurman, K. Wang, I. Kaminer, Resonant phase-matching between a light wave and a free-electron wavefunction. *Nat. Phys.* **16**, 1123–1131 (2020).
22. R. Dahan, A. Gorlach, U. Haeusler, A. Karnieli, O. Eyal, Y. Peyman, M. Sergev, A. Arie, G. Eisenstein, P. Hommelhoff, I. Kaminer, Imprinting the quantum statistics of photons on free electrons. *Science* **373**, 1324 (2021).
23. R. Shiloh, T. Chlouba, P. Hommelhoff, Quantum-coherent light-electron interaction in a scanning electron microscope. *Phys. Rev. Lett.* **128**, 235301 (2022).
24. J. Lim, S. Kumar, Y. S. Ang, L. K. Ang, L. J. Wong, Quantum interference between fundamentally different processes is enabled by shaped input wavefunctions. *Adv. Sci.* **10**, e2205750 (2023).
25. I. Kaminer, J. Nemirovsky, M. Rechtsman, R. Bekenstein, M. Segev, Self-accelerating dirac particles and prolonging the lifetime of relativistic fermions. *Nat. Phys.* **11**, 261–267 (2015).
26. G. M. Vanacore, I. Madan, F. Carbone, Spatio-temporal shaping of a free-electron wave function via coherent light–electron interaction. *Riv. Nuovo Cim.* **43**, 567–597 (2020).
27. S. V. Yalunin, A. Feist, C. Ropers, Tailored high-contrast attosecond electron pulses for coherent excitation and scattering. *Phys. Rev. Res.* **3**, L032036 (2021).
28. Z. Zhao, K. J. Leedle, D. S. Black, O. Solgaard, R. L. Byer, S. Fan, Electron pulse compression with optical beat note. *Phys. Rev. Lett.* **127**, 164802 (2021).
29. Y. Morimoto, P. Baum, Diffraction and microscopy with attosecond electron pulse trains. *Nat. Phys.* **14**, 252–256 (2018).
30. L. J. Wong, B. Freelon, T. Rohwer, N. Gedik, S. G. Johnson, All-optical three-dimensional electron pulse compression. *New J. Phys.* **17**, 013051 (2015).
31. M. Kozák, T. Eckstein, N. Schönenberger, P. Hommelhoff, Inelastic ponderomotive scattering of electrons at a high-intensity optical travelling wave in vacuum. *Nat. Phys.* **14**, 121–125 (2018a).
32. M. Kozák, N. Schönenberger, P. Hommelhoff, Ponderomotive generation and detection of attosecond free-electron pulse trains. *Phys. Rev. Lett.* **120**, 103203 (2018b).
33. J. Lim, Y. Chong, L. J. Wong, Terahertz-optical intensity grating for creating high-charge, attosecond electron bunches. *New J. Phys.* **21**, 033020 (2019).
34. J. Harris, V. Grillo, E. Mafakheri, G. C. Gazzadi, S. Frabboni, R. W. Boyd, E. Karimi, Structured quantum waves. *Nat. Phys.* **11**, 629–634 (2015).
35. V. Grillo, E. Karimi, G. C. Gazzadi, S. Frabboni, M. R. Dennis, R. W. Boyd, Generation of nondiffracting electron bessel beams. *Phys. Rev. X* **4**, 011013 (2014).

36. G. M. Vanacore, G. Berruto, I. Madan, Ultrafast generation and control of an electron vortex beam via chiral plasmonic near fields. *Nat. Mater.* **18**, 573–579 (2019).
37. E. Jones, M. Becker, J. Luiten, H. Batelaan, Laser control of electron matter waves. *Laser Photonics Rev.* **10**, 214–229 (2016).
38. H. Faresab, M. Yamada, A quantum mechanical analysis of smith–purcell free-electron lasers. *Nucl. Instrum. Methods. Phys. Res. B* **785**, 143–152 (2015).
39. N. Talebi, Schrödinger electrons interacting with optical gratings: Quantum mechanical study of the inverse smith–purcell effect. *New J. Phys.* **18**, 123006 (2016).
40. G. Guzzinati, A. Béché, H. Lourenço-Martins, J. Martin, M. Kociak, J. Verbeeck, Probing the symmetry of the potential of localized surface plasmon resonances with phase-shaped electron beams. *Nat. Commun.* **8**, 14999 (2017).
41. C. Roques-Carmes, N. Rivera, J. D. Joannopoulos, M. Soljačić, I. Kaminer, Nonperturbative quantum electrodynamics in the Cherenkov effect. *Phys. Rev. X* **8**, 041013 (2018).
42. A. Gover, Y. Pan, Dimension-dependent stimulated radiative interaction of a single electron quantum wavepacket. *Phys. Lett. A* **382**, 1550–1555 (2018).
43. Y. Pan, A. Gover, Spontaneous and stimulated radiative emission of modulated free-electron quantum wavepackets-semiclassical analysis. *J. Phys. Commun.* **2**, 115026 (2018).
44. V. Di Giulio, M. Kociak, F. J. Garcia de Abajo, Probing quantum optical excitations with fast electrons. *Optica* **6**, 1524 (2019).
45. Y. Pan, A. Gover, Spontaneous and stimulated emissions of a preformed quantum free-electron wave function. *Phys. Rev. A* **99**, 052107 (2019).
46. A. Gover, R. Ianconescu, A. Friedman, C. Emma, N. Sudar, P. Musumeci, C. Pellegrini, Superradiant and stimulated-superradiant emission of bunched electron beams. *Rev. Mod. Phys.* **91**, 035003 (2019).
47. O. Kfir, Entanglements of electrons and cavity photons in the strong-coupling regime. *Phys. Rev. Lett.* **123**, 103602 (2019).
48. O. Kfir, H. Lourenço-Martins, G. Storeck, M. Sivis, T. R. Harvey, T. J. Kippenberg, A. Feist, C. Ropers, Controlling free electrons with optical whispering-gallery modes. *Nature* **582**, 46–49 (2020).
49. A. Karnieli, N. Rivera, A. Arie, I. Kaminer, Superradiance and subradiance due to quantum interference of entangled free electrons. *Phys. Rev. Lett.* **127**, 060403 (2021).
50. A. Karnieli, N. Rivera, A. Arie, I. Kaminer, The coherence of light is fundamentally tied to the quantum coherence of the emitting particle. *Sci. Adv.* **7**, eabf8096 (2021).
51. O. Kfir, V. Di Giulio, F. J. García de Abajo, C. Ropers, Optical coherence transfer mediated by free electrons. *Sci. Adv.* **7**, 18 (2021).
52. L. J. Wong, N. Rivera, C. Murdia, T. Christensen, J. D. Joannopoulos, M. Soljačić, I. Kaminer, Control of quantum electrodynamical processes by shaping electron wavepackets. *Nat. Commun.* **12**, 1700 (2021).
53. L. W. W. Wong, X. Shi, A. Karnieli, I. Kaminer, L. J. Wong, Tailoring free electron spontaneous emission from graphene using shaped electron wavepackets, in *Conference on Lasers and Electro-Optics* (Optica Publishing Group, 2022), p. JTh5P.3.
54. G. Baranes, R. Ruimy, A. Gorlach, I. Kaminer, Free electrons can induce entanglement between photons. *NPJ Quantum Info.* **8**, 32 (2022).
55. L. J. Wong, I. Kaminer, Prospects in x-ray science emerging from quantum optics and nanomaterials. *Appl. Phys. Lett.* **119**, 130502 (2021).
56. F. Carbone, P. Musumeci, O. J. Luiten, C. Hebert, A perspective on novel sources of ultrashort electron and x-ray pulses. *Chem. Phys.* **392**, 1–9 (2012).
57. A. Ben Hayun, O. Reinhardt, J. Nemirovsky, A. Karnieli, N. Rivera, I. Kaminer, Shaping quantum photonic states using free electrons. *Sci. Adv.* **7**, eabe4270 (2021).
58. N. Talebi, I. Březinová, Exchange-mediated mutual correlations and dephasing in free-electrons and light interactions. *New J. Phys.* **23**, 063066 (2021).
59. R. Haindl, A. Feist, T. Domröse, M. Möller, S. V. Yalunin, C. Ropers, Coulomb-correlated electron number states in a transmission electron microscope beam. *Nat. Phys.* **19**, 1410–1417 (2023).
60. S. Meier, J. Heimerl, P. Hommelhoff, Few-electron correlations after ultrafast photoemission from nanometric needle tips. *Nat. Phys.* **19**, 1402–1409 (2023).
61. S. Keramati, W. Brunner, T. J. Gay, H. Batelaan, Non-poissonian ultrashort nanoscale electron pulses. *Phys. Rev. Lett.* **127**, 180602 (2021).
62. P. Hommelhoff, Y. Sortais, A. Aghajani-Talesh, M. A. Kasevich, Field emission tip as a nanometer source of free electron femtosecond pulses. *Phys. Rev. Lett.* **96**, 077401 (2006).
63. C. Ropers, D. R. Solli, C. P. Schulz, C. Lienau, T. Elsaesser, Localized multiphoton emission of femtosecond electron pulses from metal nanotips. *Phys. Rev. Lett.* **98**, 043907 (2007).
64. B. Barwick, C. Corder, J. Strohaber, N. Chandler-Smith, C. Uiterwaal, H. Batelaan, Laser-induced ultrafast electron emission from a field emission tip. *New J. Phys.* **9**, 142–142 (2007).
65. H. Yanagisawa, C. Hafner, P. Doná, M. Klöckner, D. Leuenberger, T. Greber, M. Hengsberger, J. Osterwalder, Optical control of field-emission sites by femtosecond laser pulses. *Phys. Rev. Lett.* **103**, 257603 (2009).
66. J. Vogelsang, J. Robin, B. J. Nagy, P. Dombi, D. Rosenkranz, M. Schiek, P. Groß, C. Lienau, Ultrafast electron emission from a sharp metal nanotaper driven by adiabatic nanofocusing of surface plasmons. *Nano Lett.* **15**, 4685–4691 (2015).
67. D. Bluvstein, H. Levine, G. Semeghini, T. T. Wang, S. Ebadi, M. Kalinowski, A. Keesling, N. Maskara, H. Pichler, M. Greiner, V. Vuletić, M. D. Lukin, A quantum processor based on coherent transport of entangled atom arrays. *Nature* **604**, 451–456 (2022).
68. H. Edlbauer, J. Wang, T. Crozes, P. Perrier, S. Ouacel, C. Geffroy, G. Georgiou, E. Chatzikyriakou, A. Lacerda-Santos, X. Waintal, D. C. Glattli, P. Roulleau, J. Nath, M. Kataoka, J. Splettstoesser, M. Acciai, M. C. da Silva Figueira, K. Öztas, A. Trellakis, T. Grange, O. M. Yevtushenko, S. Birner, C. Bäuerle, Semiconductor-based electron flying qubits: Review on recent progress accelerated by numerical modelling. *EPJ Quantum Technol.* **9**, 21 (2022).
69. O. Reinhardt, C. Mechel, M. Lynch, I. Kaminer, Free-electron qubits. *Ann. Phys.* **533**, 2000254 (2021).
70. S. Huang, R. Duan, N. Pramanik, J. S. Herrin, C. Boothroyd, Z. Liu, L. J. Wong, Quantum recoil in free-electron interactions with atomic lattices. *Nat. Photonics* **17**, 224–230 (2023).
71. A. Karnieli, S. Fan, Jaynes-cummings interaction between low-energy free electrons and cavity photons. *Sci. Adv.* **9**, eadh2425 (2023).
72. A. Karnieli, S. Tsesses, R. Yu, N. Rivera, A. Arie, I. Kaminer, S. Fan, Universal and ultrafast quantum computation based on free-electron-polariton blockade. *PRX Quant.* **5**, 010339 (2023).
73. M. Unternährer, B. Bessire, L. Gasparini, D. Stoppa, A. Stefanov, Coincidence detection of spatially correlated photon pairs with a monolithic time-resolving detector array. *Opt. Express* **24**, 28829–28841 (2016).
74. A. Karnieli, S. Tsesses, R. Yu, N. Rivera, Z. Zhao, A. Arie, S. Fan, I. Kaminer, Quantum sensing of strongly coupled light-matter systems using free electrons. *Sci. Adv.* **9**, eadd2349 (2023).
75. G. Huang, N. J. Engelsen, O. Kfir, C. Ropers, T. J. Kippenberg, Electron-photon quantum state heralding using photonic integrated circuits. *PRX Quant.* **4**, 020351 (2023).
76. D. Jannis, K. Müller-Caspary, A. Béché, A. Oelsner, J. Verbeeck, Spectroscopic coincidence experiments in transmission electron microscopy. *Appl. Phys. Lett.* **114**, 143101 (2019).
77. M. Aidelsburger, F. O. Kirchner, F. Krausz, P. Baum, Single-electron pulses for ultrafast diffraction. *Proc. Natl. Acad. Sci. U.S.A.* **107**, 19714–19719 (2010).
78. P. Baum, On the physics of ultrashort single-electron pulses for time-resolved microscopy and diffraction. *Chem. Phys.* **423**, 55–61 (2013).
79. S. Lahme, C. Kealhofer, F. Krausz, P. Baum, Femtosecond single-electron diffraction. *Struct. Dyn.* **1**, 034303 (2014).

Acknowledgments: S.K. thanks S. Hwang for helping proofread the manuscript. **Funding:** This project was supported by the Ministry of Education, Singapore, under its AcRF Tier 2 program (award no. MOE-T2EP50222-0012). L.J.W. acknowledges the Nanyang Assistant Professorship Start-up Grant. J.L. and L.K.A. acknowledge funding from A*STAR AME IRG (Project ID A2083c0057), MOE PhD Research Scholarship, and USA Office of Naval Research (Global) grant (Project ID N62909-19-1-2047). Y.S.A. is supported by the Singapore Ministry of Education Academic Research Fund Tier 2 (Award No. MOE-T2EP50221-0019). N.R. acknowledges support from a Junior Fellowship from the Harvard Society of Fellows. **Author contributions:** S.K. and J.L. developed the theory and performed the simulations. L.J.W., J.L., and S.K. conceived the idea and analyzed the results. S.K. and J.L. wrote the manuscript with inputs from L.J.W., N.R., W.W., Y.S.A., and L.K.A. L.J.W. supervised the project. **Competing interests:** The authors declare that they have no competing interests. **Data and materials availability:** All data needed to evaluate the conclusions in the paper are present in the paper and/or the Supplementary Materials. Code required to reproduce the results in this paper is provided in a repository at DR-NTU at: https://doi.org/10.21979/N9/UFN1SK.

Submitted 15 November 2023
Accepted 4 April 2024
Published 8 May 2024
10.1126/sciadv.adm9563